Heriot-Watt University
Research Gateway

Sol-gel spin coated well adhered MoO_3 thin films as an alternative counter electrode for dye sensitized solar cells

Citation for published version:
Mutta, GR, Popuri, SR, Wilson, JIB & Bennett, NS 2016, 'Sol-gel spin coated well adhered MoO_3 thin films as an alternative counter electrode for dye sensitized solar cells', *Solid State Sciences*, vol. 61, pp. 84-88. https://doi.org/10.1016/j.solidstatesciences.2016.08.016

Digital Object Identifier (DOI):
10.1016/j.solidstatesciences.2016.08.016

Link:
Link to publication record in Heriot-Watt Research Portal

Document Version:
Peer reviewed version

Published In:
Solid State Sciences

General rights
Copyright for the publications made accessible via Heriot-Watt Research Portal is retained by the author(s) and / or other copyright owners and it is a condition of accessing these publications that users recognise and abide by the legal requirements associated with these rights.

Take down policy
Heriot-Watt University has made every reasonable effort to ensure that the content in Heriot-Watt Research Portal complies with UK legislation. If you believe that the public display of this file breaches copyright please contact open.access@hw.ac.uk providing details, and we will remove access to the work immediately and investigate your claim.

Download date: 13. May. 2025

Sol gel spin coated well-adhered MoO_3 thin films as an alternative counter electrode for dye sensitized solar cells

Geeta R. Mutta, Srinivasa R. Popuri, John I. B. Wilson and Nick S. Bennett

School of Engineering & Physical Sciences, Heriot-Watt University, Edinburgh EH14 4AS, United Kingdom

Abstract

In this work, we aim to develop a viable, inexpensive and non-toxic material for counter electrodes in dye sensitized solar cells (DSSCs). We employed an ultra-simple synthesis process to deposit MoO_3 thin films at low temperature by sol-gel spin coating technique. These MoO_3 films showed good transparency. It is predicted that there will be 150 times reduction of precursors cost by realizing MoO_3 thin films as a counter electrode in DSSCs compared to commercial Pt. We achieved a device efficiency of about 20 times higher than that of the previous reported values. In summary we develop a simple low cost preparation of MoO_3 films with an easy to scale up process along with good device efficiency. This work encourages the discovery and development of novel and relatively new materials and paves the way for massive reduction of industrial costs which is a prime step for commercialization of DSSCs.

Key words: Molybdenum oxide, spin coating, screen printing, counter electrode, dye sensitized solar cells, photoconversion efficiency

1. Introduction

Fossil fuels have been the chief source of power generation for the human race for nearly two centuries. A consequence of which is the depletion of energy resources coupled with significant damage to the environment. Thus the energy crisis is one of the major issues to be addressed by human kind across the globe. The greatest challenge of these times is finding an inexpensive, sustainable and carbon-free renewable energy source.[1] Amongst all the renewable energy sources, solar energy is regarded as the notable means of clean energy due to its numerous advantages, which include its capability to operate without greenhouse gas emission or toxicity, quiet (no noise), along with global abundance. Hence, solar cells which convert sunlight into electricity are considered as a mainstream renewable energy resource.[2] Dye-sensitized solar cells (DSSCs) are one of the most prominent third generation solar cells, because of their low cost-to-performance ratio, simple fabrication procedures, display in various colors and semi-transparency, plasticity, function at wide angles and low-intensity incident light, light-weight and eco-friendliness. Thus DSSCs are considered as a commercially realistic solar energy-conversion solution.[3,4] Whilst DSSCs perform well at the laboratory scale, in order to commercialize these products, the three prime important factors which seek attention are efficiency, lifetime and cost.

A conventional DSSC consists of a semiconducting film, dye sensitizer, electrolyte and a counter electrode (CE). Traditionally mesoporous TiO_2 is deposited on transparent conducting oxide (TCO) coated glass substrate and the light harvesting agent which is the dye sensitizer (for example N719) is anchored to the TiO_2 film.[5] The sensitized TiO_2 serves as the photoanode. An electrolyte is typically made of a redox couple (for example iodine/ tri-iodide) dissolved in an organic solvent. The counter electrode is classically made of Platinum (Pt) film deposited on a TCO coated glass substrate. The operation principle of DSSCs is as follows: upon illumination the dye molecules anchored to TiO_2 serve to harvest light i.e. absorb light and excite electrons to lowest unoccupied molecular orbital (LUMO) levels and then injects the electrons into the conduction band of the semiconductor oxide. Theses electrons then travel through the nanoparticle network by means of diffusion to the current collector (i.e. photoanode) and eventually pass through the external circuit towards a counter electrode. Meanwhile the oxidized dye molecules are regenerated by the iodine ions from the electrolyte and the cycle is completed by reduction of tri-iodide ions in the electrolyte by the electrons reaching the counter electrode from the external load.[5] Hence for smooth functioning of the DSSC, the counter electrode plays a leading role by

reducing the redox species to regenerate the dye sensitizer. Thus catalytic activity of counter electrodes is a prerequisite along with good electrical conductivity, which justifies the classical choice of Pt.

Due to the excellent catalytic nature of Pt, it is extensively used so far in the preparation of DSSCs. The Pt being an expensive rare metal in the earth's crust, is one of the most expensive components in DSSCs which accounts for about 40% of the total manufacturing cost.[6, 7] Along with production cost, another concern is the corrosive nature of Pt with the contact of iodine liquid electrolyte, which raises the issue of long-term stability of DSSCs.[8] The aforementioned drawbacks have urged researchers to consider substitute materials to Pt. Hence to combat the production cost of DSSCs, the alternative materials for counter electrodes should satisfy the criterion of being highly catalytically active with reasonable electrical conductivity, inexpensive, non-toxic, easily available and thermally stable. To date there are many organic and inorganic materials reported in the literature. For more details the reader may refer to the following comprehensive reviews [9, 10, 11, 12]. Whilst a multitude of materials have been explored as counter electrode materials, transitional metal oxides (TMOs) are a unique class of material system which are abundant in nature, non-toxic, thermally stable, can possess good electrical conductivity along with reasonable catalytic activity. All these characteristics make TMOs a potential candidate for CEs in DSSCs. Recently TMOs have gained research attention in the context of DSSCs.[12] Some of the very recent works can be referred to elsewhere. [13, MRB, 14]

Of TMO_S, molybdenum tri-oxide (MoO_3) is one of the well-known oxide materials, known for its potential applications in diverse fields of technology such as in energy storage, catalysis, solution processable solar cells, electrochromics, photochromics, thermochromics, display materials, sensors, lubricants, etc.[15, 16,17, 18, 19, 20, 21] Even though, MoO_3 has shown to be a promising TMO in many fields, it has not yet gained major attention in DSSCs. Until now, only a single report is available on the implementation of MoO_3 as a counter electrode in DSSCs.[17] Hence there is a lot of scope to explore this material further. In this manuscript, we present an ultra-facile synthesis of MoO_3 thin films on fluorine doped tin oxide (FTO) coated glass substrates by means of sol-gel spin coating. Herein, we have employed MoO_3 as a counter electrode and it is identified as having the potential to act as a less expensive alternative counter electrode to Pt.

2. Experimental details

Sol-gel spin coating technique was used to deposit MoO_3 films on FTO coated glass substrates, as detailed in section 3.1.1. The phase conformity and crystallographic structure of MoO_3 films were investigated by automated PANalytical X' Pert Diffractometer, Netherlands (using Ni filtered Cu K_α radiation, λ= 1.5406 Å). The top view and the cross-sectional view of the surface morphology of deposited samples were observed by field emission scanning electron microscopy (Quanta 650 FEG ESEM and XL30 ESEM, respectively). The optical absorption of the film was measured by diffuse reflectance at room temperature using a Perkin Elmer Lambda 950 UV–Vis–NIR spectrophotometer. DSSC prototype devices were fabricated by sandwiching dye sensitized TiO_2 photoanodes and MoO_3 films as counter electrodes. Photovoltaic performance of these DSSCs, were carried out using an Air Mass 1.5 Global solar simulator (92250 A, Newport, USA) with an irradiation intensity of 100 mW cm^{-2}.

3. Results and discussion

3.1. Fabrication and characterization of MoO_3 film counter electrode

3.1.1. Deposition of MoO_3 films

The MoO_3 films were deposited at atmospheric pressure on FTO coated glass substrate by a low temperature solution processed sol-gel spin coating method. A step wise preparation of the MoO_3 counter electrode is shown by pictorial representation in Fig. 1.

The precursor solution was made by dissolving commercial MoO_3 powder in ammonia–water at room temperature and stirred under continuous magnetic stirring for 15 mins. At this stage, a transparent precursor solution was obtained. It is reported that this transparent solution could contain ammonium molybdate species through the following chemical reaction sequence.[22]

$$MoO_3 + 2NH_3 + H_2O \rightarrow (NH_4)_2MoO_4$$

The as prepared solution was stored in a clean and firmly closed flask and left for a whole night without disturbance. Prior to beginning deposition, the substrates were cleaned thoroughly - an important step which can govern the quality of the deposited layer and as a result, the performance of the final device. Before this step, the FTO glass substrates (Pilkington TEC glass™, sheet resistance: 11.7 Ω/sq, 2.2 mm in thickness, TEC-12) were cut into small pieces (2 × 2 cm) which then underwent a series of cleaning steps. The substrates were cleaned initially by

soapy water and then ultrasonicated for 15 mins in each of these solvents; deionised water, acetone and lastly by isopropanol. Later these substrates were dried in flowing nitrogen to remove any remains of solvent traces. After drying, a transparent adhesive tape was used to mask the substrate in such a way that a small strip of about 4 mm was masked to provide a non-coated area for electrical contacts. The spin coating was performed on these substrates so that the MoO_3 film was formed on the exposed portion of the FTO substrate. The aqueous ammonium molybdate solution was spin coated on these prepared substrates in air. The spinning driving cycles of the spin coater (SP3600) was adjusted in a series of 4 steps as follows: a spinning speed of 200 rpm for 20s, 300 rpm for 20s, 1000 rpm for 100s and 3000 rpm for 300s. All these steps went in succession and were repeated 6 times to produce a reasonable thickness of thin film. After the deposition of the final coating, the adhesive tape was removed and the underneath area was wiped using a cotton swab soaked in alcohol. Later, this precursor film was subjected to anneal at 200 ºC for 30 min in air, during which $(NH_4)_2MoO_4$ on the surface of the substrate was expected to decompose to form MoO_3 along with volatile components such as NH_3 and H_2O, and the resulting MoO_3 semi-transparent film.

To check the adherence of these MoO_3 films, the film was covered with scotch tape and removed. We did not notice any visual damage to the film. To check the mechanical stability of these films, we ultrasonicated these MoO_3 spin coated films for 15 mins in acetone and no visible changes in the film were observed. This demonstrated that the resulting MoO_3 coatings were well adhered on FTO coated glass substrates. These spin coated annealed films were subjected to structural and optical characterizations and DSSC devices were fabricated utilizing MoO_3 films as the counter electrode, and the photoconversion efficiency was evaluated.

3.1.2. Structural and optical characterization of MoO_3 films

X-Ray diffraction studies

In order to study the phase formation of spin coated films, we carried out an X-ray diffraction (XRD) structural study at room temperature. The X-ray diffraction patterns for the non-annealed and annealed spin coated thin film samples, along with a simulated MoO_3 XRD pattern are presented in Fig. 2. Except the reflections from the underlying FTO substrates, as-deposited MoO_3 films didn't exhibit any kind of Bragg reflections (blue solid line in Fig. 2), indicating the

amorphous nature of these films. Upon annealing at 200 °C for 30 min, several diffraction reflections emerged, which indicates the crystallization of these thin films (red solid line in Fig. 2). All these diffraction reflections can be assigned to the thermodynamically stable orthorhombic α phase of MoO_3. For comparison, a simulated standard diffraction pattern of α-MoO_3 using JCPDS card no: 005-0508 is also shown with a black solid line in Fig. 2. Although, α phase of MoO_3 exists in lamellar structure, striking preferential orientation of thin films are not clearly visible from XRD patterns.[23] Furthermore, no other peaks of impurities were observed, indicating the phase purity of deposited α-MoO_3 thin films. Using Le Bail profile matching analysis, XRD data was indexed with orthorhombic crystal system with space group Pbnm (62) and lattice parameters are calculated as a= 3.952 (3) Å, b= 13.863 (2) Å, c= 3.714 (2) Å and V= 203.47 (2) $Å^3$.[24] These lattice parameters are in excellent agreement with α-MoO_3 phase.[25]

Morphological study by FESEM

The surface morphologies of precursor MoO_3, bare FTO substrates, as deposited films and annealed films were examined using scanning electron microscopy (SEM) and representative micrographs of each of them are exemplified in Fig. 3. Fig. 3a shows the top view of the commercial FTO glass which consists of many grains with different shapes and sizes. The grain sizes are ca. 100-600 nm. Commercial MoO_3 morphology consists of belt-like anisotropic crystals, as shown in Fig. 3b. The typical length of these micro-belts was in the range of 1 to 100 μm and ~ 5–15 μm in width. Fig. 3c and 3d demonstrate the surface morphology of spin-coated MoO_3 followed by thermal treatment at 200 °C for 30 min. Fig. 3c displays the morphology of spin coated amorphous MoO_3 film which is a seamless pattern of 'wrinkled structures' with an average dimension of a few tens of μm. Each wrinkled structure is composed of more than one or two tiny structures, which look like individual 'tree branches'. Each branch in this tiny unit is connected to the other one with a central core. The inset figure in Fig. 3c gives a closer view of one of these structures. It is also noticed that the substrate is well covered by the deposited film. Fig. 3d shows the morphology of air-annealed MoO_3 thin films resembles 'wood grain texture' or a ridged surface, where the inset shows the close up view. The surface homogeneity of the annealed film is relatively better and appears to be smoother than that of the as deposited one. This shows the annealing favoured the formation of crystalline MoO_3 films, which is in line with XRD

measurements. The annealed thin films were estimated from cross-sectional SEM to have a thickness of ~ 1.4 to 2.2 µm.

Optical absorption spectra

The optical properties of spin coated MoO_3 films were investigated from UV–Vis–NIR spectro-photometric measurements. The optical reflectance spectra of these films were recorded at room temperature in diffused reflectance mode in the wavelength range 250 to 800 nm. In order to obtain the percentage of reflectance solely from the MoO_3 film, it was necessary to normalize the reflectance for FTO coated glass substrates. It can be seen from Fig. 4 inset that the reflectivity of the annealed film in the visible region is about 27 %, i. e. ca. 73 % transparent. It is observed that these films shows a strong absorption around 350-450 nm. We have also calculated the optical band gap of the films using the reflectance spectra. By utilizing Tauc relation[ref] for direct band gap transition, we have estimated the optical band gap of MoO_3 film in Fig. 4, which is about 3.14 eV. The obtained bang gap is close to the reported values earlier in the literature on MoO_3 material[ref?].

3.2. Fabrication of MoO_3 CE DSSCs and Photovoltaic characterization

3.2.1. Fabrication of prototype DSSC devices

The N719 dye sensitized TiO_2 photoelectrodes were fabricated by screen printing method on FTO substrates of the same grade as that used for preparing counter electrodes. The complete stepwise procedure of preparing these photoelectrodes can be seen in ref.[13] These freshly prepared sensitized photoelectrodes and counter electrodes were assembled into a sandwich type cell to fabricate a prototype DSSC. In brief, both electrodes were put together in a way that the active side of sensitized titania was facing the MoO_3 counter electrode. While clubbing these electrodes, special care had to be taken to shift the glass plates in order to leave a space at the end of each electrode for electrical contacts. To hold properly, both of these electrodes were fastened using paper binder clips. Later the liquid electrolyte which was composed of 0.05 M Iodine, 0.1 M lithium iodine, 0.6 M 1-butyl-3-methylimidazolium iodide and 0.5 M 4-tertbutyl pyridine in a mixture of acetonitrile and valeronitrile, was drawn into the space between the electrodes by capillary action. Any excess electrolyte was wiped off with a cotton swab and the final device was ready to be measured for photoconversion efficiency. The assembled device schematic is shown in Fig. 5.

3.2.2. Photovoltaic characterization of DSSCs

The photovoltaic parameters of the final assembled DSSC device has been investigated by analyzing the current density (J)–voltage (V) curve. The J-V measurements were performed under the light illumination of 100 mW cm^{-2} (AM1.5G), with an active cell area of 0.25 cm^2. Fig. 6 display the J–V curve of a fabricated DSSC with the MoO_3-based counter electrode. The photoconversion efficiency (η) of the DSSC was extracted from the J-V curve by utilizing the following equations

$$\eta = \left(\frac{V_{oc} \times J_{sc} \times FF}{P_{in}}\right) \times 100$$

$$FF = \left(\frac{V_{max} \times J_{max}}{V_{oc} \times J_{sc}}\right)$$

where J_{sc} represents the photocurrent density, V_{oc} is the open-circuit voltage, FF is the fill factor and P_{in} is the intensity of incident light. V_{max} and J_{max} are the maximum voltage and current density for the maximum power output.

The spin coated MoO_3 film CE DSSC showed a solar to electrical energy conversion efficiency of ~ 1.04 %, with the J_{sc} of 8.17 $mAcm^{-2}$, V_{oc} of 0.70 V and FF of 16.59 %. These results are 20 times higher in magnitude than that of TCO-free DSSCs fabricated by Kovendham et al.[17] The high value of J_{sc} in our case, might be related to the higher reduction of tri-iodide ions in the electrolyte, over the MoO_3 film based CE since it is known that the reduction of tri-iodide ions in redox electrolyte is associated with the electrocatalytic properties of the counter electrode. It is worth mentioning that the MoO_3 film is well adhered onto FTO substrate, in other words, it provides a good contact with the substrate which eventually helps the transfer of electrons. In the case of standard Pt-based sealed type DSSCs fabricated in our lab, typically we acquire a power conversion efficiency of ~ 7 %.[13, MRB] In the present study our MoO_3-CE based DSSCs show a lower performance compared to Pt CE-based DSSCs, however we achieve the aim of introducing/developing new materials to offer an alternative to replace the expensive Pt. It is to be noted that the stability evaluation of the device over time was not a subject of our present study, as the DSSC device assembly is open to ambient air, though the device functions until the electrolyte solvent evaporates. It is clear the performance of the cell will deteriorate with time. However, there lies a significant amount of lifetime to measure and determine the photovoltaic output of the as fabricated DSSC. We believe there is still a plenty of room to optimize MoO_3 thin

films and eventually to enhance the efficiency of MoO_3 CE based DSSCs. Our future work is in progress to ascertain the optimum parameters of MoO_3 films such as film thickness, annealing temperature, annealing time and morphology tuning. Along with optimization of synthesis and device parameters, we intend to check the suitability of this CE with alternative dyes and redox mediators, which will help us to pin-point the best possible combination of these to enhance the device efficiency in combination with the stability.

4. Conclusion

Earth abundant, cheap, environmentally safe and scalable materials are of huge interest to substitute the high-priced Pt in DSSCs. In this manuscript, we report the facile synthesis of MoO_3 thin films on FTO substrates, the combination of which has been explored as a counter electrode in DSSCs. Here, we adopted the sol-gel spin coating deposition technique to fabricate MoO_3 thin films, which has good possibility for scale up for large area DSSC fabrication. The obtained thin film has been confirmed in terms of phase purity by XRD and it possesses homogeneous morphology all over the film, with high transparency. Our first results demonstrate a photoconversion efficiency of MoO_3 counter electrode DSSCs of 1.04 %, which is about 20 times higher than existing reports. The current MoO_3 thin film is far from being optimized, but allows for the feasibility of future enhancement of MoO_3 thin films as counter electrodes in DSSCs, particularly given the interesting prospect of the sol-gel approach in terms of scalability.

Acknowledgements

Dr. Jim Buckman of Heriot-Watt University and Dr. Vasundhara of NIIST-CSIR laboratory are gratefully acknowledged for the access to SEM and XRD facilities, respectively.

References

[1] Nilofar Asim, Kamaruzzaman Sopian, Shideh Ahmadi, Kasra Saeedfar, MA Alghoul, Omidreza Saadatian, and Saleem H Zaidi, Renewable and Sustainable Energy Reviews **16** (8), 5834 (2012).
[2] Bhubaneswari Parida, S_ Iniyan, and Ranko Goic, Renewable and sustainable energy reviews **15** (3), 1625 (2011).
[3] Anders Hagfeldt, Gerrit Boschloo, Licheng Sun, Lars Kloo, and Henrik Pettersson, Chemical reviews **110** (11), 6595 (2010).
[4] Qifeng Zhang, Kwangsuk Park, Junting Xi, Daniel Myers, and Guozhong Cao, Advanced Energy Materials **1** (6), 988 (2011).
[5] Jiawei Gong, Jing Liang, and K Sumathy, Renewable and Sustainable Energy Reviews **16** (8), 5848 (2012).
[6] Greg Smestad, Carlo Bignozzi, and Roberto Argazzi, Solar energy materials and solar cells **32** (3), 259 (1994).
[7] Karuppannan Rokesh and Alagarsamy Pandikumar, presented at the Materials Science Forum, 2014 (unpublished).
[8] RJ Dawson and GH Kelsall, ECS Electrochemistry Letters **2** (11), D55 (2013).
[9] Jayaraman Theerthagiri, Arumugam Raja Senthil, Jagannathan Madhavan, and Thandavarayan Maiyalagan, ChemElectroChem **2** (7), 928 (2015).
[10] Meidan Ye, Xiaoru Wen, Mengye Wang, James Iocozzia, Nan Zhang, Changjian Lin, and Zhiqun Lin, Materials Today **18** (3), 155 (2015).
[11] Mingxing Wu and Tingli Ma, The Journal of Physical Chemistry C **118** (30), 16727 (2014).
[12] Mingxing Wu, Xiao Lin, Yudi Wang, Liang Wang, Wei Guo, Daidi Qi, Xiaojun Peng, Anders Hagfeldt, Michael Grätzel, and Tingli Ma, Journal of the American Chemical Society **134** (7), 3419 (2012).
[13] Geeta R Mutta, Srinivasa R Popuri, Michal Maciejczyk, Neil Robertson, M Vasundhara, John IB Wilson, and Nick S Bennett, Materials Research Express **3** (3), 035501 (2016).
[14] Jian WeiáGuo and Hua GuiáYang, Chemical Communications **49** (53), 5945 (2013).
[15] Yuping Chen, Chunliang Lu, Lin Xu, Ying Ma, Wenhua Hou, and Jun-Jie Zhu, CrystEngComm **12** (11), 3740 (2010).
[16] Claudio Girotto, Eszter Voroshazi, David Cheyns, Paul Heremans, and Barry P Rand, ACS applied materials & interfaces **3** (9), 3244 (2011).
[17] M Kovendhan, D Paul Joseph, P Manimuthu, S Ganesan, P Maruthamuthu, S Austin Suthanthiraraj, C Venkateswaran, and R Mohan, presented at the American Institute of Physics Conference Series, 2011 (unpublished).
[18] SB Patil, SR Mane, VR Patil, RR Kharade, and BN Bhosale, Archiv Appl Sci Res **3**, 481 (2011).
[19] K Bange, Solar Energy Materials and Solar Cells **58** (1), 1 (1999).
[20] Mohammad Bagher Rahmani, Sayyed-Hossein Keshmiri, J Yu, AZ Sadek, L Al-Mashat, A Moafi, K Latham, YX Li, W Wlodarski, and K Kalantar-Zadeh, Sensors and Actuators B: Chemical **145** (1), 13 (2010).
[21] Jianfang Wang, Kai C Rose, and Charles M Lieber, The Journal of Physical Chemistry B **103** (40), 8405 (1999).
[22] PS Patil and RS Patil, Bulletin of Materials Science **18** (7), 911 (1995).
[23] PF Carcia and EM McCarron, Thin Solid Films **155** (1), 53 (1987).
[24] Juan Rodríguez-Carvajal, Physica B: Condensed Matter **192** (1), 55 (1993).

[25] Angamuthuraj Chithambararaj, N Rajeswari Yogamalar, and A Chandra Bose, Crystal Growth & Design **16** (4), 1984 (2016).

Figure 1. Schematic illustration of the preparation of MoO_3 films supported on an FTO coated glass substrate using sol-gel spin coating technique.

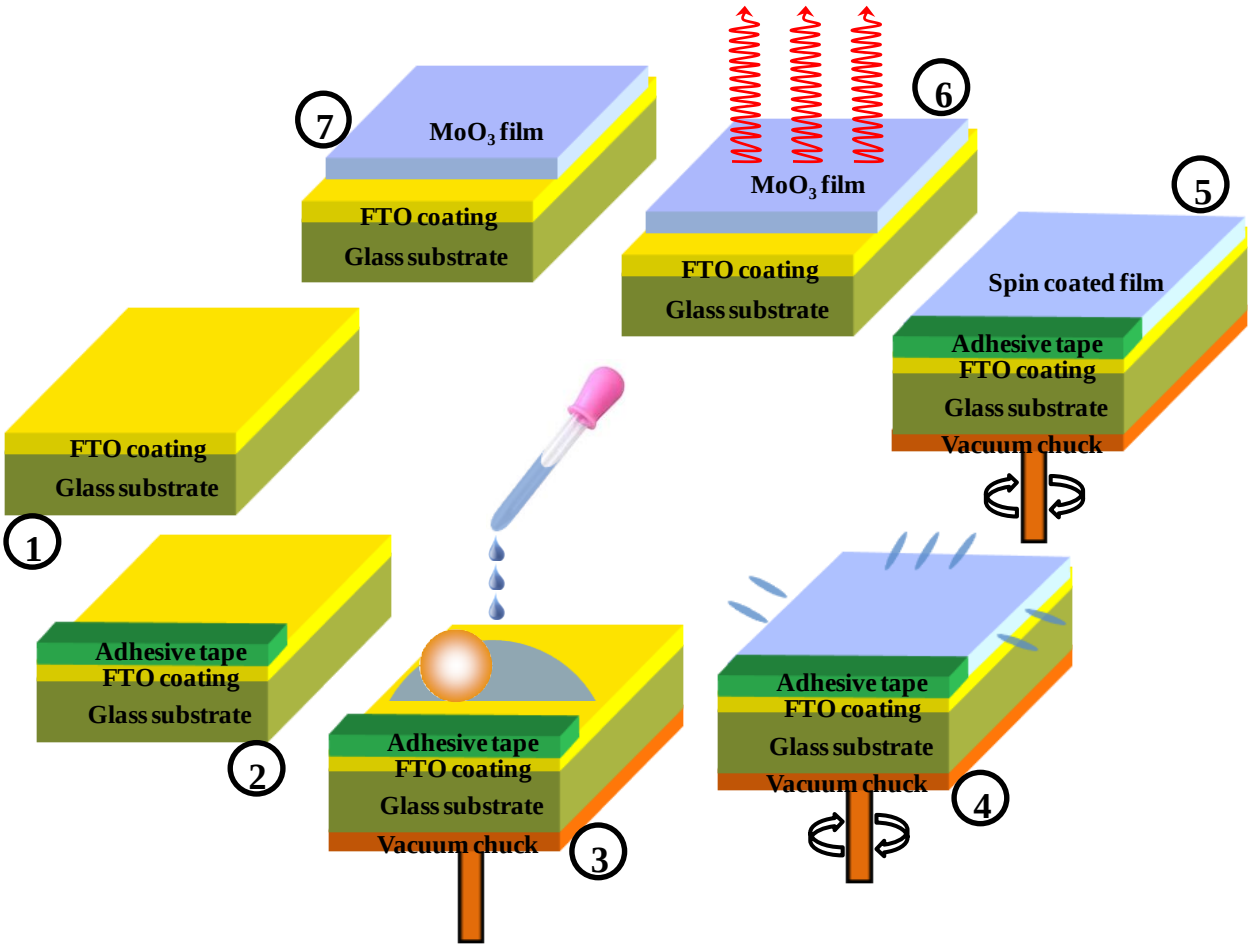
FTO coating
Glass substrate
1
Adhesive tape
FTO coating
Glass substrate
2
Adhesive tape
FTO coating
Glass substrate
Vacuum chuck
3
Adhesive tape
FTO coating
Glass substrate
Vacuum chuck
4
Spin coated film
Adhesive tape
FTO coating
Glass substrate
Vacuum chuck
5
MoO3 film
FTO coating
Glass substrate
6
MoO3 film
FTO coating
Glass substrate
7

Figure 2. Powder XRD patterns of annealed and non-annealed MoO_3 film along with simulated pattern.

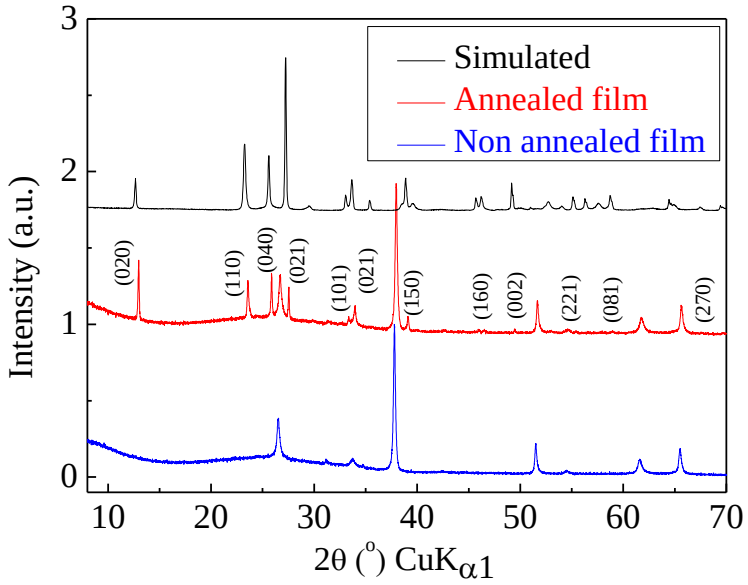

Figure 3. SEM images of (a) Bare FTO coated glass substrate, (b) Commercial MoO_3 powder, (c) Non-annealed MoO_3 surface and, (d) Annealed MoO_3 surface.

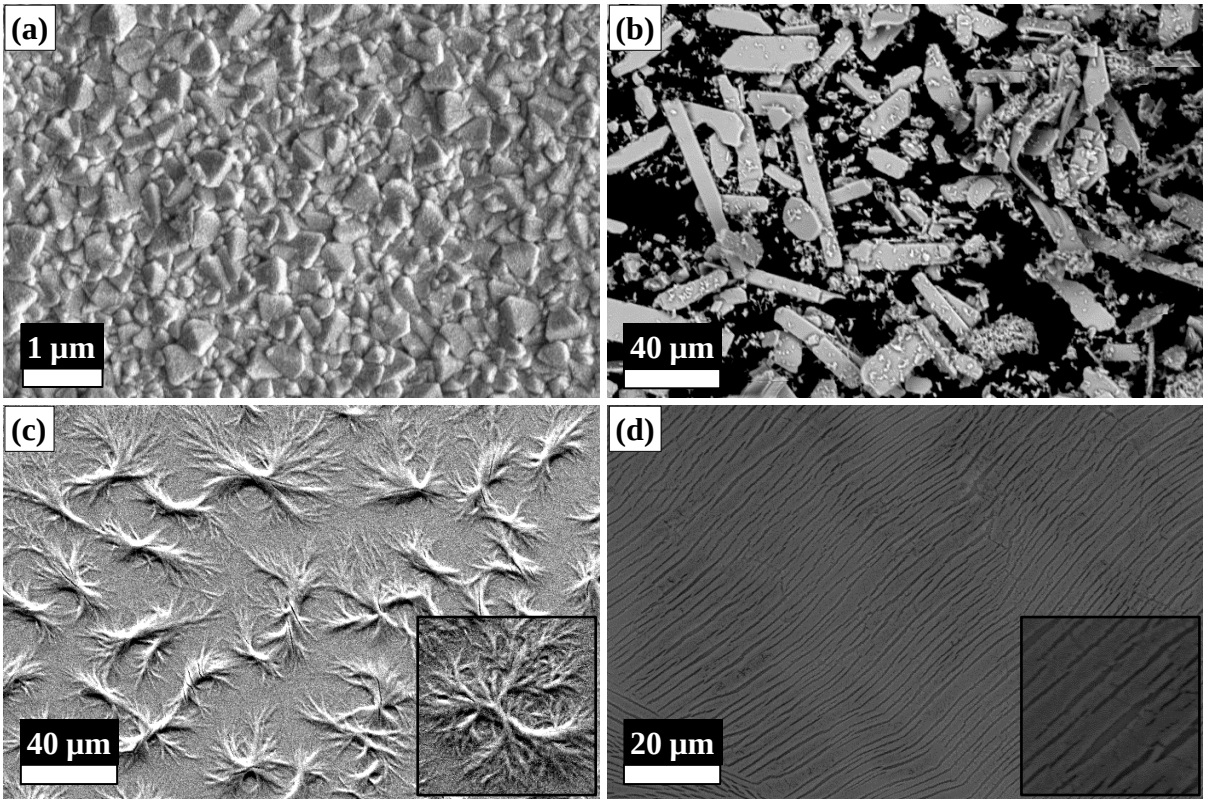

Figure 4. Plot to estimate the direct optical band gap of annealed MoO_3 spin coated films. Inset figure shows the graph of reflectance vs. wavelength.

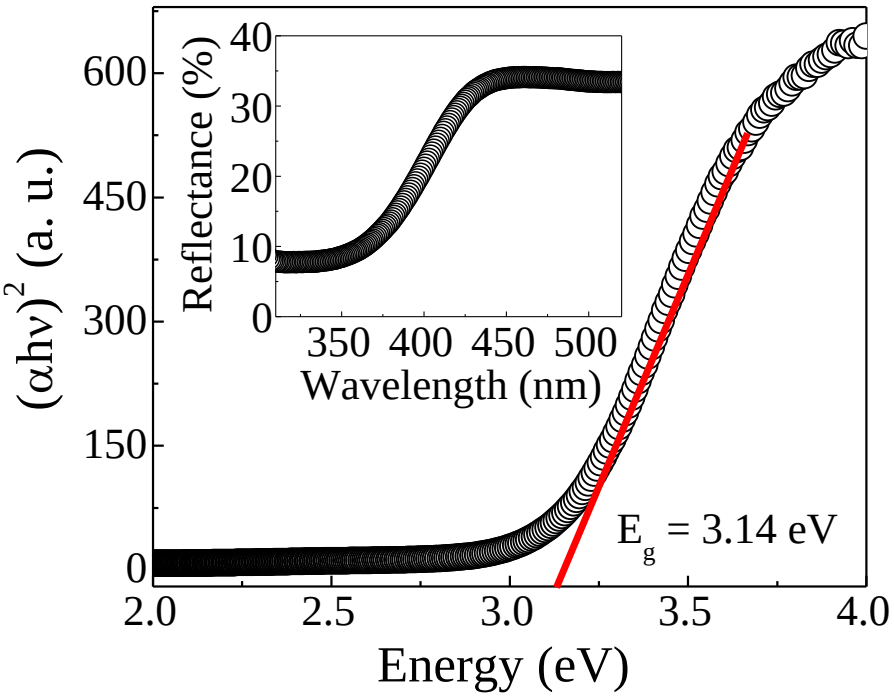

Figure 5. Schematic device structure of DSSC prepared in this study, the final MoO_3 spin coated film supported on FTO glass used as the counter electrode and TiO_2 as the photoanode.

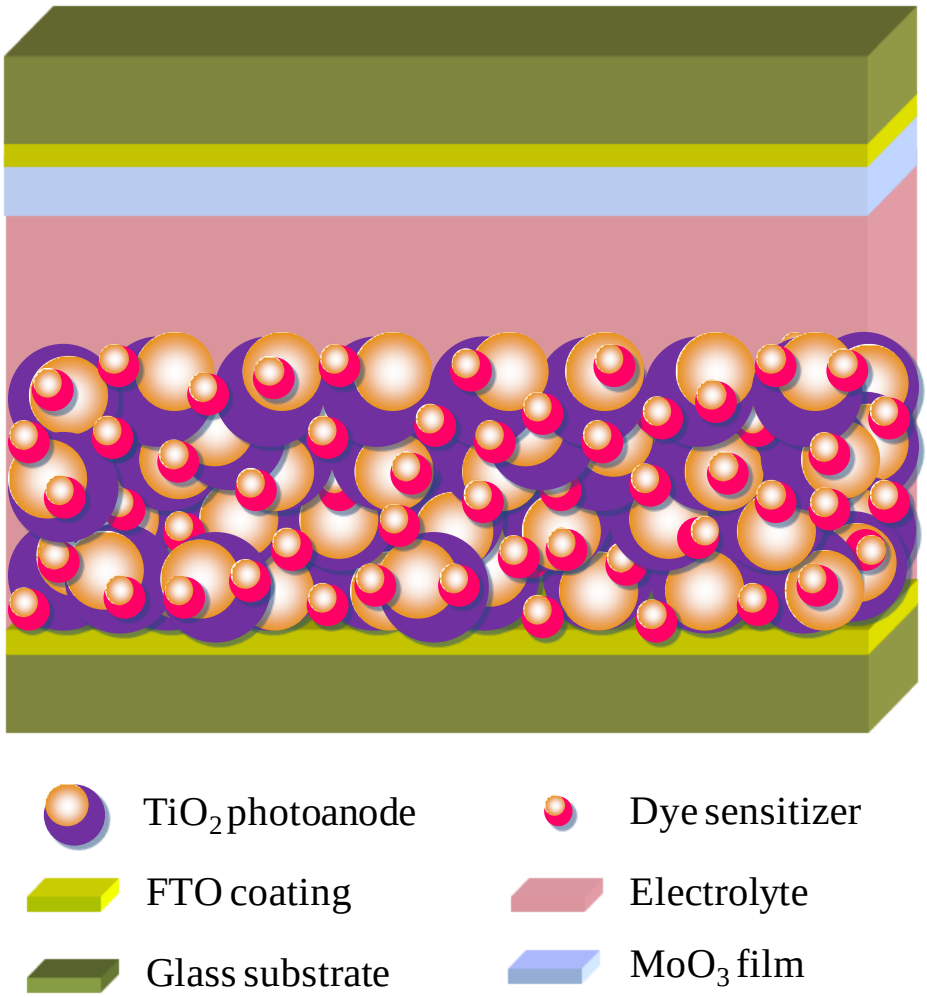

Figure 6. J-V curve of the DSSCs fabricated with MoO_3 spin coated film supported on FTO glass as the counter electrode.